Piezometric level variations and ground deformations in the plain of the Sarno River (southern Italy)

Silvio Coda[1], Domenico Calcaterra[1], Delia Cusano[1], Salvatore Davino[2], Diego Di Martire[1] & Vincenzo Allocca[1]

[1]Department of Earth Sciences, Environment and Resources, University of Naples Federico II.
[2]IdroGeo S.r.l.

SC, 0000-0003-2744-4771; DC, 0000-0002-3480-3667; DC, 0000-0002-6751-7990; DDM, 0000-0003-0046-9530; VA, 0000-0001-7146-2438.

Rend. Online Soc. Geol. It., Vol. 66 (2025), pp. 44-49, 4 figs. https://doi.org/10.3301/ROL.2025.09

Short Note

Corresponding author e-mail: silvio.coda@unina.it

Citation: Coda S., Calcaterra D., Cusano D., Davino S., Di Martire D. & Allocca V. (2025) - Piezometric level variations and ground deformations in the plain of the Sarno River (southern Italy). Rend. Online Soc. Geol. It., 66, 44-49, https://doi.org/10.3301/ROL.2025.09.

Guest Editor: Guido Leone

Submitted: 15 January 2025
Accepted: 31 March 2025
Published online: 10 April 2025

SOCIETÀ GEOLOGICA ITALIANA ETS
FONDATA NEL 1881 - ENTE MORALE R. D. 17 OTTOBRE 1885

ABSTRACT

Variations in piezometric levels due to natural and anthropogenic factors can cause vertical ground deformations, often with significant consequences for urban environments. This study investigates the pyroclastic-alluvial aquifer of the Sarno Plain (southern Italy) to analyze piezometric level changes and ground deformations at basin and local scales, covering the periods 1978–2021 and 1993–2020, respectively. A GIS-based hydrogeological database was developed, integrating piezometric and hydrostratigraphic data from literature, local archives, and new field surveys. Ground deformations were assessed using Differential Interferometry SAR (DInSAR) data from four constellations, with mean displacement rate maps and time series generated through the DInSAR technique. At the basin scale, four sectors showed the largest piezometric variations, with drawdowns exceeding -10 m and rises up to +8 m. Subsidence was prevalent across wide portions of the plain, with rates exceeding -10 mm/yr, while uplift occurred mostly in scattered, localised areas. In four selected areas—two experiencing piezometric drawdown and subsidence, and two with piezometric rise and uplift—time series comparisons highlighted a good correspondence between piezometric changes and ground deformation. Moreover, local hydrostratigraphic conditions influenced the deformative response, with the largest displacements observed under phreatic aquifer conditions and in areas with compressible peaty and clayey layers.

KEYWORDS: piezometric variations, subsidence, uplift, DInSAR, southern Italy.

INTRODUCTION

Ground deformations associated with fluctuations in groundwater levels have been recognised on a global scale, posing georisk to human activities and urban settlements in certain instances (Tang et al., 2022; Yang et al., 2019). The quantitative characterisation of hydrogeological basins, along with the natural and anthropogenic processes involved, is crucial for the proper management of groundwater resources and their use in fresh-water supply (Alberti et al., 2022; UN Water, 2022). Conversely, mismanagement of groundwater resources exacerbates hydrogeological imbalances, often resulting in overexploitation, and subsidence induced by groundwater extraction is well-documented in the scientific literature (Galloway, 2013; Guzy & Malinowska, 2020; Pacheco-Martínez et al., 2013). This phenomenon is mostly related to aquifer compaction for reduction in pore pressure (Liu et al., 2019). On the other hand, uncontrolled cessation of pumping can trigger groundwater rebound phenomena (Allocca et al., 2022), causing piezometric levels to recover and possible ground uplift (Chen et al., 2007; Coda et al., 2019a; Teatini et al., 2011). Moreover, several studies reported the occurrence of uplift for rising of piezometric levels due to water injection (Teatini et al., 2011) and artificial groundwater recharge (Zhang et al., 2015).

Currently, the most commonly used approaches to address ground deformations induced by piezometric variations resort to remote sensing for deformation monitoring and to geotechnical modelling (Guzy & Malinowska, 2020). In particular, satellite technologies offer significant advantages over in situ measurements, enabling scientists to conduct regional-scale mapping and monitor ground deformation more cost-effectively (Tomás et al., 2014). Among these technologies, the DInSAR technique is particularly widespread for understanding the spatial extent and temporal evolution of such phenomena (Bonì et al., 2016; Coda et al., 2019b; Tessitore et al., 2016; Vilardo et al., 2009).

In this study, the piezometric variation and vertical ground deformation, both negative and positive, were analyzed in the pyroclastic alluvial aquifer of the Sarno River plain (southern Italy) at both basin and local scales. Several studies conducted in specific sectors of this area highlighted the cause-effect relationship between groundwater depletion induced by pumping and subsidence (Fabbrocino et al., 2007), as well as subsidence due to a combination of natural and anthropogenic factors (Valente et al., 2021). Over the last 20 years, changes in land and groundwater use have led to sector-specific rises in piezometric levels. Therefore, the evolution of piezometric levels from 1978 to 2021 was reconstructed using historical piezometric data and a new hydrogeological campaign. Ground deformation was detected using DInSAR data covering the period from 1993 to 2020. In addition to reconstructing updated piezometric and deformative trends at the scale of the whole hydrogeological basin of the Sarno River plain, the study aimed to analyze the deformative response across four sectors of the aquifer in relation to the magnitude of piezometric variation and local hydrostratigraphic characteristics.

STUDY AREA

The Sarno River plain (Fig. 1a) is a coastal pyroclastic alluvial plain that extends for about 170 km^2. It is the southern extension of the Campanian plain and is bordered to the west by the Somma-Vesuvius volcanic complex, to the east by the carbonate reliefs of the Sarno Mts. and Lattari Mts. and it is separated to the north-west from other sectors of the Campanian plain by both a morphological and underground watershed. Morphology of study area is essentially flat with altitude variable between 0 and 70 m a.s.l. in the plan sectors, while values up to 325 m a.s.l. are reached in the limited piedmont areas.

From a hydrogeological point of view, on a basin scale, there is a single underground groundwater body (De Vita et al., 2018), albeit characterised by marked heterogeneity and anisotropy mainly due to the presence of a discontinuous tuffaceous aquitard attributable to the Campanian Ignimbrite eruption (Phlegraean Fields; 39ky) (Ducci et al., 2012).

Aquifer recharge occurs not only through direct infiltration but also via transfers from the Somma-Vesuvius aquifer, Sarno Mts. and Lattari Mts. carbonate hydrostructures that border the plain (Celico, 1983; Petrone et al., 2024). In the two carbonate aquifers, there are several tapping works for drinking water purposes (Petrone et al., 2024), both gravity-fed and through wells, located near the boundary with the plain. The plain is highly urbanised, with urban areas and industrial sites covering about 70% of its surface; the remaining part is predominantly agricultural.

DATA AND METHODS

Stratigraphic and piezometric data

Figure 1b shows the flowchart of the methodological approach adopted for this study. The first step was the development of a GIS-based hydrogeological database, including 165 stratigraphic logs (ubications are reported into supplementary materials) obtained from national databases, local administration archives, technical and scientific works, and seven piezometric contour maps sourced from the scientific literature. These maps correspond to the periods September 1978 (Celico, 1983), April 1992 (Celico & Piscopo,

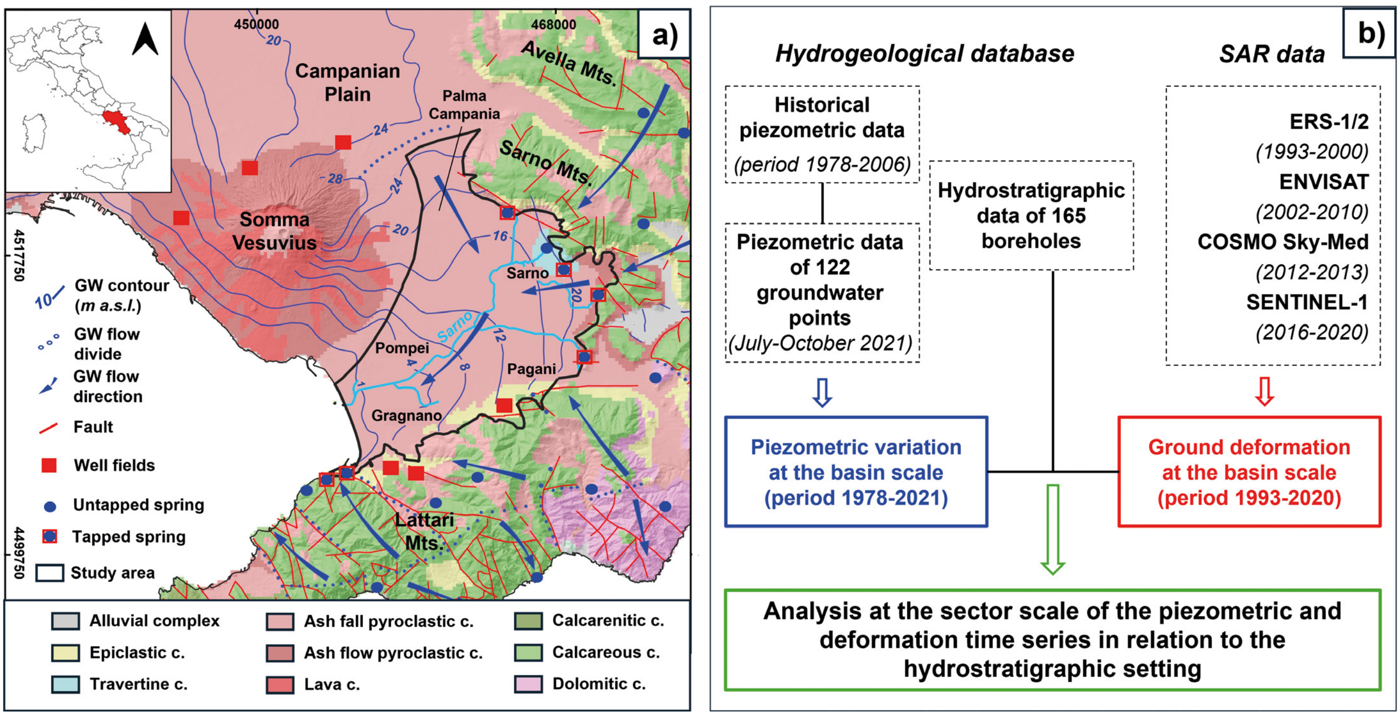

Fig. 1 - (a) Hydrogeological map of study area (modified after De Vita et al., 2018) and (b) flowchart of the adopted approach for this study.

1995), March and May 2003, April and September 2005, and April 2006 (Termolini, 2007). The contours were digitised and rasterised in the ArcMap environment (ESRI, version 10.8).

A new hydrogeological campaign was conducted in September 2021, during which 122 groundwater points (piezometers, wells, and draining surface water bodies) were measured using Global Navigation Satellite System (GNSS) and a water-level dipper. Hydraulic heads were interpolated using the Empirical Bayesian Kriging (EBK) method (Gribov & Krivoruchko, 2020) via the Geostatistical Analyst tool implemented in ArcMap software (ESRI, version 10.8).

Piezometric variation at the basin scale was evaluated by calculating differences between the raster pair representing the entire period (1978–2021), and the sectors with the highest drawdown or rise were identified to reconstruct the local hydrostratigraphic setting and piezometric hydrographs considering the eight piezometric scenarios (i.e, September 1978, April 1992, March and May 2003, April and September 2005, April 2006, and September 2021).

Interferometric data and displacement analysis

DInSAR data provide ground deformation measurements for each satellite acquisition date, projected along the Line of Sight (LoS) direction. This enables the generation of mean displacement rate maps and time series. In this study, SAR data were obtained and processed as part of the Italian First and Third Not-ordinary Plan of Environmental Remote Sensing project, under a specific agreement with the Italian Ministry of Environment (MATTM). Specifically, 138 images captured by the ERS-1/2 satellites (66 images in ascending geometry and 72 in descending geometry), 105 images from the ENVISAT satellite (65 in ascending geometry and 40 in descending geometry), 35 descending images from COSMO-SkyMed, and 105 ascending images from Sentinel-1 were utilised. These datasets cover the monitoring periods of 1993–2000, 2002–2010, 2012–2013, and 2016–2020, respectively, and were processed using the DInSAR technique.

Finally, for the comparative analysis of piezometric and deformation time series at the sector scale, the Permanent Scatter (PS) points located within the representative areas of high piezometric variations were considered.

RESULTS AND DISCUSSION

Piezometric variation and ground deformation

The updated groundwater flow scheme is shown in figure 2a, reconstructed based on the hydrogeological campaign conducted in September 2021. The maximum piezometric levels, reaching

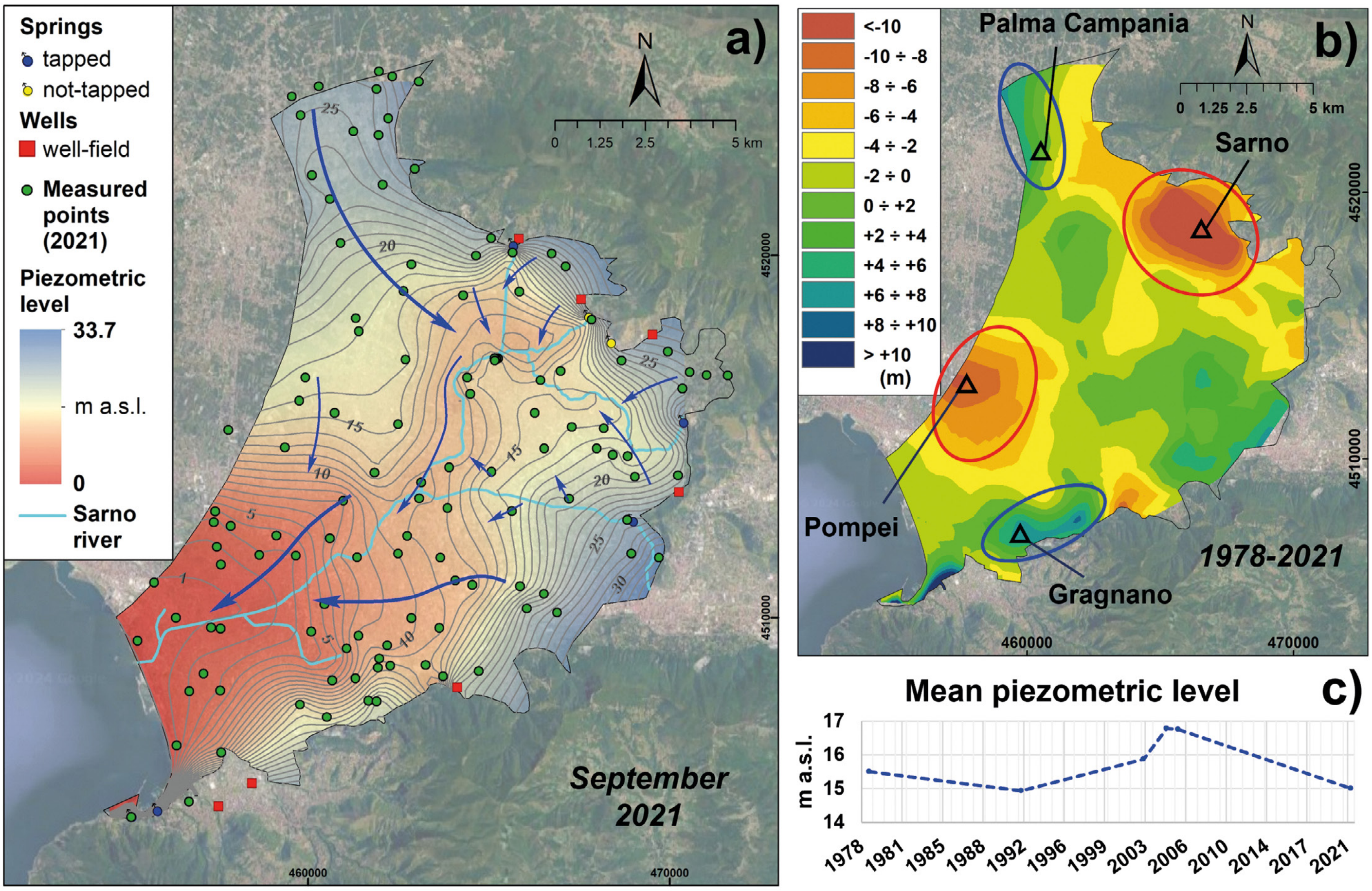

Fig. 2 - (a) Piezometric map relative to the period September 2021 (piezometric contours are in grey and values are expressed in m a.s.l.), (b) piezometric variation for the period 1978-2021, and (c) evolution of the mean piezometric level.

up to 33.7 m a.s.l., are observed at the north-eastern and eastern margins of the plain. The hydraulic gradient is highly variable, reflecting the heterogeneity of the aquifer. The Sarno River confirms its role as a drainage feature, acting as a preferential groundwater flow direction in the inner sector of the plain.

The analysis of piezometric variations at the basin scale over the entire period (1978–2021; Fig. 2b) reveals that approximately 70% of the area is experiencing drawdown, with four sectors characterised by the most significant changes. The north-eastern (Sarno area) and south-western (Pompei area) margins show drawdown values greater than -10 meters. In these sectors, the drawdown is attributed to the presence of several active industrial sites with high pumping rates. In contrast, two sectors exhibit rising values up to +8 meters at the north-western margin (Palma Campania area) and the southern margin (Gragnano area), where intermittent reductions in pumping rates for industrial and drinking water use have occurred, triggering a groundwater rebound phenomenon similar to that observed in the adjacent hydrogeological basin of the eastern plain of Naples (Allocca et al., 2022). Based on the available data, the evolution of mean piezometric levels at the basin scale can be divided into three main phases (Fig. 2c): a decline period between 1978 and 1992, a rising phase up to the first half of the 2000s, and a subsequent decline continuing until 2021.

Figure 3 shows the mean displacement rate maps for the considered satellites and the respective periods. In general, negative rates prevail over positive ones, with values greater than -10 mm/yr, indicating extensive sectors affected by subsidence. This phenomenon has also been documented by other authors (Fabbrocino et al., 2007; Valente et al., 2021), who primarily attributed it to pumping activities and the natural compaction of compressible sediments. Specifically, in the north-eastern sector (corresponding to the Sarno area) and in the inner part of the plain along the NE-SW direction, subsidence is observed across all acquisition periods, except in the COSMO-SkyMed map (Fig. 3c), which shows a slight uplift (up to +5 mm/yr) during the 2012–2013 period. Additional evidence of widespread uplift is highlighted in the western sector, as detected by the ERS satellite in descending

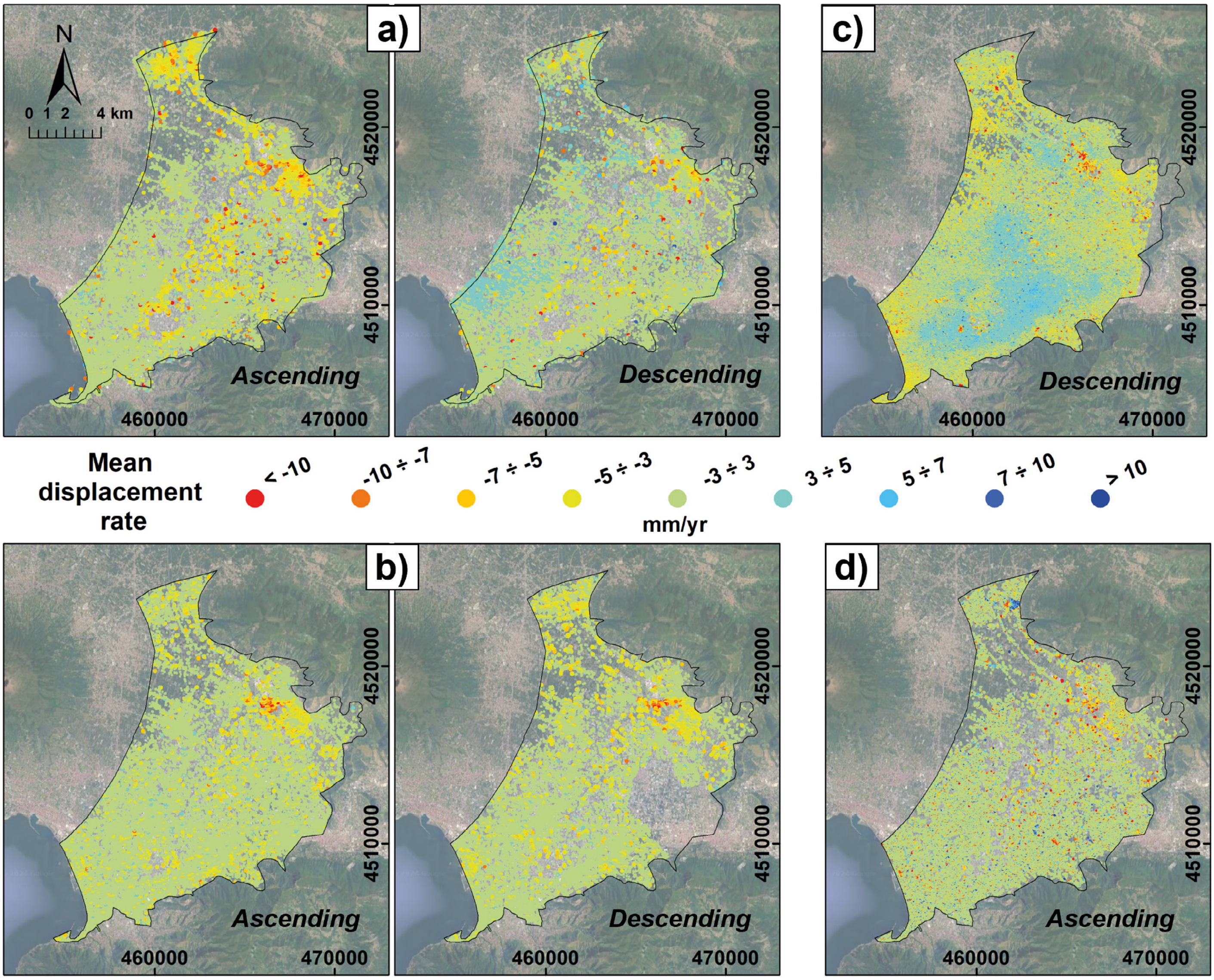

Fig. 3 - Mean displacement rate maps relative to (a) ERS 1/2 (1993-2000 period), (b) ENVISAT (2002-2010 period), (c) COSMO-SkyMed (2012-2013 period), and (d) Sentinel-1 (2016-2020 period) constellations.

geometry (Fig. 3a). For the ENVISAT (Fig. 3b) and Sentinel-1 (Fig. 3d) satellites, positive rates are more localised and display a scattered distribution.

Integrated analysis of ground deformation

Comparing the time series of piezometric levels and LOS displacements in the four selected areas (Fig. 4), a clear correspondence between piezometric and deformation trends is observed, suggesting a cause-effect relationship between piezometric variations and ground deformations. This relationship is further supported by previous studies (Fabbrocino et al., 2007; Valente et al., 2021). In detail, the areas affected by piezometric rise, related to the groundwater rebound phenomenon, and ground uplift (Palma Campania and Gragnano areas) exhibit different deformation responses. In the Gragnano area, a maximum piezometric rise of +4.7 m corresponds to a deformation of +45 cm, whereas in the Palma Campania area, a smaller piezometric rise (+2.9 m) results in a LOS displacement of +119 cm. As observed in other sectors of the Campanian Plain (Coda et al., 2019b), local hydrostratigraphic conditions strongly influence the deformation rates. The Palma Campania area is characterised by incoherent pyroclastic deposits and phreatic aquifer conditions, which enable greater elastic deformability compared to the Gragnano area, where the aquifer is semi-confined by Campanian Ignimbrite tuff. The presence of highly compressible layers significantly influences subsidence rates in areas affected by piezometric drawdown. Specifically, the Sarno area experiences greater subsidence (-192 cm) compared to the Pompei area (-82 cm), with piezometric drawdowns of -14.4 m and -9.2 m, respectively. Both areas exhibit phreatic conditions, but the higher subsidence observed in the Sarno area is attributed to the high compressibility of its peaty and clayey layers, rather than solely to the magnitude of the drawdown.

CONCLUSIONS

This study reconstructs the piezometric evolution of the coastal pyroclastic alluvial aquifer of the Sarno Plain during the period 1978–2021, based on literature data and new field surveys. It also analyzes ground deformations detected using SAR data. The multiscale analysis provides a preliminary characterisation of the ground's deformative response to piezometric variations, considering local hydrostratigraphic settings; in the four selected sectors of the study area, the highest negative and positive LOS displacements are detected in correspondence of highly compressible layers and phreatic condition of the aquifer. The developed hydrogeological database and the obtained results represent a basis for further studies aimed at investigating the causes of piezometric variations and the associated deformative mechanisms.

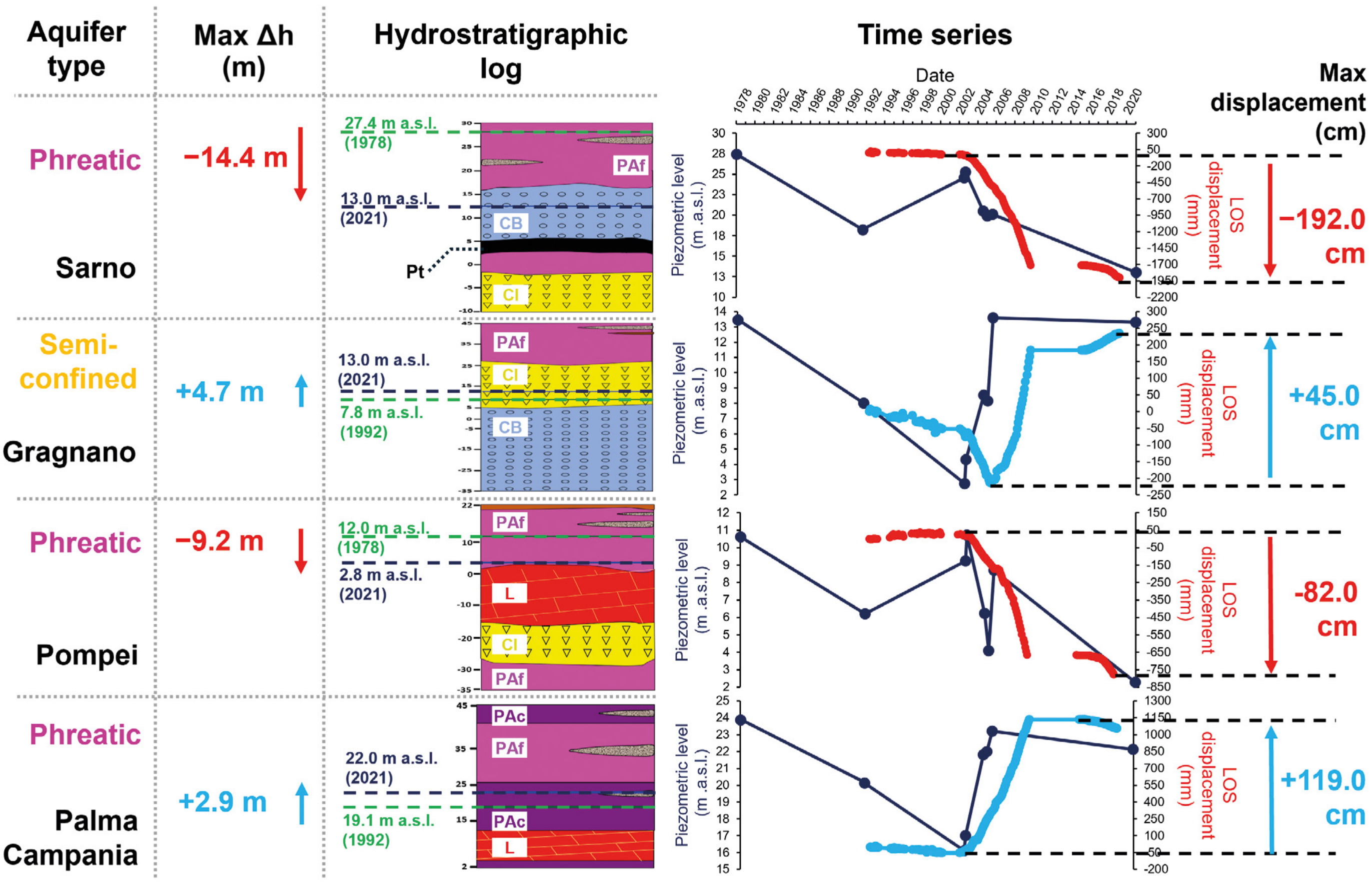

Fig. 4 - Comparison between hydrostratigraphic characteristics and time series of piezometric levels and LOS displacements in the four selected sectors. Hydrostratigraphic layers: fine (PAf) and medium-coarse (PAc) pyroclastic, marine and alluvial deposits; carbonate conglomerate, breccias and debris (CB); peats and clays (Pt); fractured lavas (L); Campanian Ignimbrite tuff (CI).

ACKNOWLEDGEMENTS

This work was carried out within the RETURN Extended Partnership and received funding from the European Union Next-GenerationEU (National Recovery and Resilience Plan – NRRP, Mission 4, Component 2, Investment 1.3 – D.D. 1243 2/8/2022, PE0000005), CUP UNINA: E63C22002000002.

REFERENCES

Alberti L., Antelmi M., Oberto G., La Licata I. & Mazzon P. (2022) - Evaluation of Fresh Groundwater Lens Volume and Its Possible Use in Nauru Island. Water, 14(20), Article 20, https://doi.org/10.3390/w14203201.

Allocca V., Coda S., Calcaterra D. & De Vita P. (2022) - Groundwater rebound and flooding in the Naples' periurban area (Italy). J. Flood Risk Manag., 15(2), Article 2, https://doi.org/10.1111/jfr3.12775.

Bonì R., Cigna F., Bricker S., Meisina C. & McCormack H. (2016) - Characterisation of hydraulic head changes and aquifer properties in the London Basin using Persistent Scatterer Interferometry ground motion data. J. Hydrol., 540, 835-849, https://doi.org/10.1016/j.jhydrol.2016.06.068.

Celico F. & Piscopo V. (1995) - Idrodinamica sotterranea e vulnerabilità all'inquinamento delle piane del Sarno e del Solofrana (Campania). Quad. Geol. Appl., 2, 407-414.

Celico P. (1983) - Idrogeologia dei massicci carbonatici, delle piane quaternarie e delle aree vulcaniche dell'Italia centro-meridionale: Marche e Lazio meridionali, Abruzzo, Molise e Campania: Vol. Quaderni della Cassa per il Mezzogiorno (4/2).

Chen C.-T., Hu J.-C., Lu C.-Y., Lee J.-C. & Chan Y.-C. (2007) - Thirty-year land elevation change from subsidence to uplift following the termination of groundwater pumping and its geological implications in the Metropolitan Taipei Basin, Northern Taiwan. Engin. Geol., 95(1), Article 1, https://doi.org/10.1016/j.enggeo.2007.09.001.

Coda S., Confuorto P., De Vita P., Di Martire D. & Allocca V. (2019) - Uplift Evidences Related to the Recession of Groundwater Abstraction in a Pyroclastic-Alluvial Aquifer of Southern Italy. Geosciences, 9(5), Article 5, https://doi.org/10.3390/geosciences9050215.

Coda S., Tessitore S., Di Martire D., Calcaterra D., De Vita P. & Allocca V. (2019) - Coupled ground uplift and groundwater rebound in the metropolitan city of Naples (southern Italy). J. Hydrol., 569, 470-482, https://doi.org/10.1016/j.jhydrol.2018.11.074.

Ducci D., De Simone S. & Sellerino M. (2012) - 3D lithostratigraphic model as support for development of a groundwater flow model: The Sarno plain (Italy) case study. Ital. J. Engin. Geol. Environm., 1, 41-58.

Fabbrocino S., Lanari R., Celico P., Termolini G. & Zeni G. (2007) - Groundwater pumping and land subsidence in the Sarno river plain (Campania). Mem. Descr. Carta Geol. d'It., 76, 163-174.

Galloway D.L. (2013) - Subsidence Induced by Underground Extraction. In P. T. Bobrowsky (Ed.), Encyclopedia of Natural Hazards (pp. 979-986). Springer Netherlands, https://doi.org/10.1007/978-1-4020-4399-4_336.

Gribov A. & Krivoruchko K. (2020) - Empirical Bayesian kriging implementation and usage. Sci. Tot. Environm., 722, 137290, https://doi.org/10.1016/j.scitotenv.2020.137290.

Guzy A. & Malinowska A. (2020) - State of the Art and Recent Advancements in the Modelling of Land Subsidence Induced by Groundwater Withdrawal. Water, 12(7), Article 7, https://doi.org/10.3390/w12072051.

Liu Y., Li J. & Fang Z.N. (2019) - Groundwater Level Change Management on Control of Land Subsidence Supported by Borehole Extensometer Compaction Measurements in the Houston-Galveston Region, Texas. Geosciences, 9(5), Article 5, https://doi.org/10.3390/geosciences9050223.

Pacheco-Martínez J., Hernandez-Marín M., Burbey T.J., González-Cervantes N., Ortíz-Lozano J.Á., Zermeño-De-Leon M.E. & Solís-Pinto A. (2013) - Land subsidence and ground failure associated to groundwater exploitation in the Aguascalientes Valley, México. Engin. Geol., 164, 172-186, https://doi.org/10.1016/j.enggeo.2013.06.015.

Petrone P., De Vita P., Marsiglia P., Allocca P., Coda S., Cusano D., Lepore D. & Allocca V. (2024) - Hydrogeological conceptual model and groundwater recharge of Avella Mts. karst aquifer (southern Italy): A literature review and update. J. Hydrol.: Reg. St., 54, 101871, https://doi.org/10.1016/j.ejrh.2024.101871.

Tang W., Zhao X., Motagh M., Bi G., Li J., Chen M., Chen H. & Liao M. (2022) - Land subsidence and rebound in the Taiyuan basin, northern China, in the context of inter-basin water transfer and groundwater management. Rem. Sens. Environm., 269, 112792, https://doi.org/10.1016/j.rse.2021.112792.

Teatini P., Gambolati G., Ferronato M., Settari A. & Walters D. (2011) - Land uplift due to subsurface fluid injection. J. Geodyn., 51(1), Article 1, https://doi.org/10.1016/j.jog.2010.06.001.

Termolini G. (2007) - Analisi degli effetti indotti dal sovrasfruttamento degli acquiferi di pianura: Emungimenti e subsidenza nella piana campana. [PhD Dissertation, University of Naples Federico II], http://dx.doi.org/10.6092/UNINA/FEDOA/2686.

Tessitore S., Fernández-Merodo J.A., Herrera G., Tomás R., Ramondini M., Sanabria M., Duro J., Mulas J. & Calcaterra D. (2016) - Comparison of water-level, extensometric, DInSAR and simulation data for quantification of subsidence in Murcia City (SE Spain). Hydrogeol. J., 24(3), 727-747, https://doi.org/10.1007/s10040-015-1349-8.

Tomás R., Romero R., Mulas J., Marturià J.J., Mallorquí J.J., Lopez-Sanchez J.M., Herrera G., Gutiérrez F., González P.J., Fernández J., Duque S., Concha-Dimas A., Cocksley G., Castañeda C., Carrasco D. & Blanco P. (2014) - Radar interferometry techniques for the study of ground subsidence phenomena: A review of practical issues through cases in Spain. Environmental Earth Sciences, 71(1), 163-181, https://doi.org/10.1007/s12665-013-2422-z.

UN Water (Ed.) (2022) - Groundwater making the invisible visible. UNESCO.

Valente E., Allocca V., Riccardi U., Camanni G. & Di Martire D. (2021) - Studying a Subsiding Urbanized Area from a Multidisciplinary Perspective: The Inner Sector of the Sarno Plain (Southern Apennines, Italy). Rem. Sens., 13(16), Article 16, https://doi.org/10.3390/rs13163323.

Vilardo G., Ventura G., Terranova C., Matano F. & Nardò S. (2009) - Ground deformation due to tectonic, hydrothermal, gravity, hydrogeological, and anthropic processes in the Campania Region (Southern Italy) from Permanent Scatterers Synthetic Aperture Radar Interferometry. Rem. Sens. Environm., 113(1), Article 1, https://doi.org/10.1016/j.rse.2008.09.007.

Yang J., Cao G., Han D., Yuan H., Hu Y., Shi P. & Chen Y. (2019) - Deformation of the aquifer system under groundwater level fluctuations and its implication for land subsidence control in the Tianjin coastal region. Environm. Monit. Assessm., 191(3), Article 3, https://doi.org/10.1007/s10661-019-7296-4.

Zhang Y., Wu J., Xue Y., Wang Z., Yao Y., Yan X. & Wang H. (2015) - Land subsidence and uplift due to long-term groundwater extraction and artificial recharge in Shanghai, China. Hydrogeol. J., 23(8), Article 8, https://doi.org/10.1007/s10040-015-1302-x.